

Large Deflection Response and Buckling of Partially and Fully Loaded Spherical Caps

NICHOLAS PERRONE*

Office of Naval Research, Washington, D.C.

AND

ROBERT KAO†

The Catholic University of America, Washington, D.C.

The Marguerre equations governing the finite deflections of spherical caps are adopted in the form of three equilibrium equations with u , v , and w , the usual displacement quantities, which are also the dependent variables in the differential equations. The equations are solved for different load situations using a finite difference nonlinear relaxation technique. A number of axisymmetric problems are solved including the following: a) uniformly loaded cap, b) "cosine" loaded cap, and c) uniformly loaded cap with clamped apex region. Complete response solutions are presented up to and including instability for two asymmetric problems—the quarter and semicircular (uniformly) loaded clamped caps. The results indicate that the smaller the load area, the lower the associated buckling pressure. An important finding is that the finite difference approximation to the ∇^4 operator is grossly inaccurate in the vicinity of the pole for asymmetric problems. A general remedy is suggested.

Introduction

DURING the last decade the spherical cap problem has been the subject of numerous investigations. A primary aim of much of the research on this problem has been to determine the buckling load of the spherical cap and, toward that end, to reconcile discrepancies between experimental and analytical results.

We might break up spherical cap problem solutions into three categories—axisymmetric, axisymmetric with perturbation techniques to obtain asymmetric solutions, and direct asymmetric solutions. Examples of studies for the axisymmetric case include Ref. 1 for point loads and uniform loads, Ref. 2 for thermal effects, Ref. 3 for the effects of initial imperfections, and Ref. 4 for the inclusion of dynamic effects.

In the second category, situations are considered wherein linear asymmetric deformations are superposed on the nonlinear axisymmetric solution to determine asymmetric buckling loads.^{5,6} We could place in the same category attempts to set up auxiliary linear differential equations as corrections on the axisymmetric solutions for the purpose of obtaining asymmetric solutions.⁷

The third category, a direct solution of the asymmetric spherical cap problem, includes a variety of significantly different attempts to solve the problem such as the following: energy techniques, a combination finite difference Fourier series approach where the functions are expanded in a Fourier series in the circumferential direction,⁸ and a complete finite difference approach to solve the governing equations.¹⁰ Matrix displacement techniques have also been used effectively.^{11,12} A combination finite difference energy/Newton's method could also be cited.¹³

Although these samplings from the literature are by no means complete, they do give a rough indication of the attempts at the title problem that have been made. Undoubtedly, the first two categories have been the ones where the bulk of the research work has been concentrated.

Received October 20, 1969; revision received April 16, 1970.

* Director, Structural Mechanics Program; on leave as N.I.H. Special Research Fellow, Georgetown University, Department of Biophysics; also Adjunct Professor of Mechanics, The Catholic University of America. Associate Fellow AIAA.

† Research Assistant, Department of Civil Engineering and Mechanics.

The spherical cap problem has been a particularly interesting one to examine because it presents a considerable number of mathematical challenges as well as significant difficulties in the interpretation of the physics of the results. It is inherently a nonlinear problem due to the effect of large deformations, and a wide variety of numerical methods have been attempted to solve the problem.

In the present case a significantly different method is brought to bear to solve spherical cap problems in the first and third categories, namely axisymmetric and direct asymmetric solutions. We will term the technique a nonlinear finite difference relaxation method.

While no one has ever attempted, to the knowledge of the authors, to establish a list of criteria that a good or an optimal numerical method should have, it would appear that the following should be almost axiomatic:

- 1) The method should be versatile, i.e., applicable to a wide variety of problems with virtually no modifications.
- 2) It should be simple conceptually so that one could grasp the essence of the approach with little difficulty.
- 3) The people time consumed in applying the method should be an absolute minimum relative to competitive methods. (People time includes time necessary to learn, apply and plan the application of the method, programming for computer as well as checking.)
- 4) Computer time should also be less than that for competitive methods; however, this is a secondary factor. Computer time decreases exponentially in cost so that this factor has a probably diminishing importance. People time, of course, is like entropy; it only increases with time.

We do believe that the method described herein to solve the spherical cap problem is an optimal one. The present example constitutes the first one in mechanics where this method is applied via computer use. Although other unpublished results have been presented with respect to the large deformations of flat membranes,¹⁴ the present paper represents the first published version of any solutions using computerized nonlinear relaxation techniques in mechanics.

Many years ago Southwell did solve some nonlinear problems utilizing relaxation techniques.¹⁵ However, in his solutions Southwell essentially utilized standard linear relaxation techniques and iterated many times to obtain his solutions. Nonlinear terms, for example, were placed on the right-hand

side of the equation and the operator, which consisted of the differential quantities, on the left-hand side was linear. After many iterations (some successful and some not so) a solution might evolve.

Shaw and Perrone introduced truly nonlinear relaxation operators and solved the flat membrane problem directly in this manner.¹⁶ The technique utilized was extremely time consuming and certainly not readily adaptable for hand calculations. With the advent of high-speed computers these methods do indeed become very competitive with other techniques to solve nonlinear problems.

In the next section the governing equations will be enumerated. This will be followed by a discussion of the solution method in fair detail. In the fourth section a number of example problems will be solved. In the next section comparisons with other solutions will be made. The final section contains a discussion and conclusions.

Governing Equations

The equations utilized governing the response of the spherical cap will be those derived by Marguerre and put in the form of displacements by Famili and Archer.¹⁰ These equations are reproduced from Ref. 10 as Eqs. (1-3).

$$\bar{u}'' + \frac{\bar{u}'}{x} - \frac{\bar{u}}{x^2} + \frac{(1-\nu)}{2} \frac{\bar{u}}{x^2} + \frac{1+\nu}{2} \frac{\bar{v}'}{x} - \frac{(3-\nu)}{2} \frac{\bar{v}}{x^2} + \bar{w}' \left[(1+\nu) \frac{\lambda^2}{m^2} + \bar{w}'' \right] + \frac{(1-\nu)}{2} \left(\frac{\bar{w}''^2}{x} + \frac{\bar{w}'\bar{w}''}{x^2} \right) + \frac{1+\nu}{2} \frac{\bar{w}}{x} \left(\frac{\bar{w}}{x} \right)' = 0 \quad (1)$$

$$\frac{1-\nu}{2} \left(\bar{v}'' + \frac{\bar{v}'}{x} - \frac{\bar{v}}{x^2} \right) + \frac{\bar{v}}{x^2} + \frac{1+\nu}{2} \frac{\bar{u}'}{x} + \frac{(3-\nu)}{2} \frac{\bar{u}}{x^2} + \frac{\bar{w}}{x} \left[(1+\nu) \frac{\lambda^2}{m^2} + \frac{1-\nu}{2} \bar{w}'' + \frac{\bar{w}}{x^2} \right] + \bar{w}' \left(\frac{1+\nu}{2} \frac{\bar{w}'}{x} + \frac{1-\nu}{2} \frac{\bar{w}}{x^2} \right) = 0 \quad (2)$$

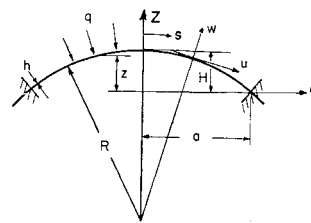
$$\nabla^4 \bar{w} + \frac{m^2 \lambda^2}{1-\nu} \left(\frac{\bar{u}}{x} + \bar{u}' + \frac{\bar{v}}{x} + \frac{2\lambda^2}{m^2} \bar{w} \right) + \frac{\lambda^2 m^2}{2(1-\nu)} \left(\bar{w}''^2 + \frac{\bar{w}^2}{x^2} \right) - 12 \nabla^2 \bar{w} \left[\frac{\bar{u}}{x} + \frac{\bar{v}}{x} + \frac{\lambda^2}{m^2} \bar{w} + \frac{1}{2} \frac{\bar{w}^2}{x^2} + \nu \left(\bar{u}' + \frac{\lambda^2}{m^2} \bar{w} + \frac{1}{2} \bar{w}''^2 \right) \right] + 12(1-\nu) \bar{w}'' \left[\frac{\bar{u}}{x} - \bar{u}' + \frac{\bar{v}}{x} - \frac{1}{2} \bar{w}''^2 + \frac{1}{2} \frac{\bar{w}^2}{x^2} \right] - 12(1-\nu) \left[\frac{\bar{u}}{x} + \bar{v}' - \frac{\bar{v}}{x} + \frac{\bar{w}'\bar{w}}{x} \right] \left(\frac{\bar{w}'}{x} - \frac{\bar{w}}{x^2} \right) = - \frac{4\lambda^4}{m^2} p(x, \theta) \quad (3)$$

where u, v and w are the tangential, circumferential and normal deflections, respectively. Pertinent nondimensional terms are given in Eqs. (4) and associated dimensions in Fig. 1;

$$\begin{aligned} x &= r/a, z = (a^2 - r^2)/2R, m^4 = 12(1-\nu^2) \\ q_{cr} &= 4Eh^2/R^2m^2, \lambda^2 = m^2a^2/Rh, p(x, \theta) = -q(x, \theta)/q_{cr} \\ ()' &= \partial/\partial x(), ()^* = \partial/\partial \theta(), \bar{u} = au/h^2, \bar{v} = av/h^2 \\ \bar{w} &= w/h, \nabla^2 = ()'' + (1/x)()' + (1/x^2)()^* \end{aligned} \quad (4)$$

Since the shell is shallow there is no difference between the dimension r which runs perpendicular to the z direction and s , a coordinate running along the shell. Other quantities of interest are as follows: h = shell thickness, E, ν are material constants, $q(x, \theta)$ = normal loading. As noted in Eqs. (4) a

Fig. 1 Geometry and notation for spherical shell.



dot over a symbol denotes differentiation with respect to θ and a prime denotes differentiation with respect to x .

Boundary conditions at the outer portion of the spherical cap are assumed to be clamped. These are enumerated as follows: $\bar{u} = \bar{v} = \bar{w} = \partial \bar{w}/\partial x = 0$.

The Marguerre equations are nonlinear because the strain displacements from which they are derived are nonlinear with respect to the normal displacement w . This nonlinearity is manifested in Eqs. (1-3) via quadratic or higher-order terms in w that appear at various points in all three equations. The equations are indeed difficult enough to attempt a solution without this nonlinearity; of course, the effect of the nonlinearity is to cause even greater difficulty in any attempt to effect a numerical solution.

Solution Method—Nonlinear Finite Difference Relaxation

Briefly, a solution is obtained by converting the governing Eqs. (1-3) into finite difference form and utilizing a nonlinear relaxation procedure to solve the resulting set of algebraic equations. In Ref. 10 Famili and Archer also used a finite difference technique to formulate the problem but the resulting algebraic equations were solved by a completely different approach. Since the solution of the equations represents the heart of the difficulty, the difference between the two approaches constitutes the essence of the problem.

A polar coordinate type finite difference mesh is superposed on the cap domain. Looking at a portion of the cap end on we would see the mesh in the vicinity of the center and boundary as shown in Fig. 2. The nodal points of the mesh would consist of the intersections of the spokes or radial lines with the concentric circles. (The coordinates describing nodal points denote the circle and spoke locations, respectively.)

The finite difference scheme for a polar coordinate mesh (e.g., Fig. 2) is very similar to that of a rectangular mesh; complexity of the former case may arise near the pole. Here, the construction of finite difference equations up to second derivatives at the inner most circle of Fig. 2 is given in Eq. (5);

$$w'(1, j) = (1/2\delta_x) \{w(2, j) - w[1, j + (M/2)d_i]\} \quad (5a)$$

$$w''(1, j) = (1/\delta_x^2) \{w(2, j) - 2w(1, j) + w[1, j + (M/2)d_i]\} \quad (5b)$$

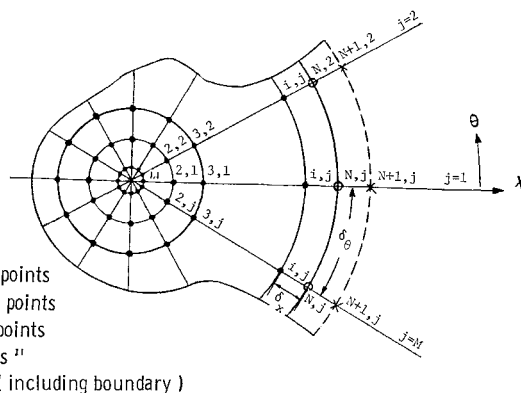


Fig. 2 Finite difference mesh on polar coordinates.

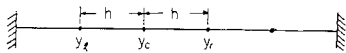


Fig. 3 One-dimensional mesh for Eq. $y'' = K$.

$$\dot{w}(1,j) = (1/2\delta_\theta)[w(1,j+1-b_i) - w(1,j-1+a_i)] \quad (5c)$$

$$\ddot{w}(1,j) = (1/\delta_\theta^2)[w(1,j+1-b_i) - 2w(1,j) + w(1,j-1+a_i)] \quad (5d)$$

$$\dot{w}'(1,j) = (1/4\delta_x\delta_\theta)[w(2,j+1-b_i) - w(1,j+1+M/2-c_i) + w(1,j-1+(M/2)e_i d_i) - w(2,j-1+a_i)] \quad (5e)$$

where $a_i = M$ when $j = 1$ and $a_i = 0$ when $j = 2, \dots, M$; $b_i = 0$ when $j = 1, 2, \dots, M-1$ and $b_i = M$ when $j = M$; $c_i = 0$ when $j = 1, 2, \dots, M/2-1$ and $c_i = M$ when $j = M/2, \dots, M$; $d_i = 1$ when $j = 1, 2, \dots, M/2$ and $d_i = -1$ when $j = M/2+1, \dots, M$; $e_i = 1$ when $j = 1, 2, \dots, M/2$ and $e_i = -1$ when $j = M/2+1$ and $e_i = 1$ when $j = M/2+2, \dots, M$.

We shall attempt to now outline the relaxation procedure in a straight-forward but schematic form. Visualize the finite equivalents of Eqs. (1-3) rewritten in such a way that all terms in the equations appear on the right hand side so that the left-hand side of all three equations should be zero. If for some mesh point, say c , we have not found the correct solution for these equations, then instead of zeros on the left hand side we would have an error term or residual as shown in Eqs. (6-8)

$$R_{cu} = f_u \quad (6)$$

$$R_{cv} = f_v \quad (7)$$

$$R_{cw} = f_w \quad (8)$$

corresponding to Eqs. (1-3), respectively; f_u, f_v , and f_w denote the right-hand sides of the finite difference forms of Eqs. (1-3).

Our problem is to develop a systematic procedure to reduce these residuals to acceptable levels. The relaxation operator for point c may be determined for the u, v or w equations by differentiating Eqs. (6-8), respectively, with respect to their appropriate functions as shown in Eqs. (9-11)

$$dR_{cu}/du_c = \partial f_u/\partial u_c = C_u = \text{const} \quad (9)$$

$$dR_{cv}/dv_c = \partial f_v/\partial v_c = C_v = \text{const} \quad (10)$$

$$dR_{cw}/dw_c = \partial f_w/\partial w_c = \text{variable} \quad (11)$$

f_u and f_v are both linear functions of u and v ; as such, the derivatives with respect to the u_c or v_c terms in Eqs. (9-10) must

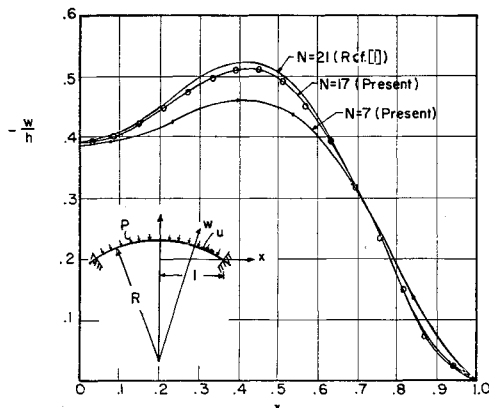


Fig. 4 Geometry of spherical shell under uniform load and comparison of normal deflection with $N = 7$ and $N = 17$ with the results in Ref. 1, with $N = 21$, $p = 0.7$, $\lambda = 6$, $\nu = \frac{1}{3}$.

both be constant quantities. f_w , on the other hand, is a non-linear function of w so that the derivatives of this function with respect to w_c is not a constant, Eq. (11). The fact that the right-hand side of Eq. (11) is not a constant indicates that the relaxation operator for the w term is approximate. This same procedure was utilized by Shaw and Perrone¹⁶ in the analysis of a large deflection flat membrane problem.

Perhaps the reasoning associated with the results of Eqs. (6-11) could better be illustrated by a very simple example, Fig. 3. Here we have a one dimensional simple finite difference mesh which is being utilized to attempt an approximate solution to the simple equation shown in the caption for Fig. 3. At each typical point c the finite difference equivalent of the differential equation could be written as shown in Eq. (12)

$$R_c = (y_r - 2y_c + y_t)/h^2 - K \quad (12)$$

Equation (12) is a simple counterpart to any of Eqs. (6-8). The relaxation operator similar to (9-11) is found by a straight-forward differentiation, Eq. (13);

$$dR_c/dy_c = -2/h^2 \quad (13a)$$

$$dR_c = -(2/h^2)dy_c \quad (13b)$$

Once the relaxation operator is known we have a systematic tool to reduce errors gradually to zero and subsequently obtain our solution to the finite difference equations. (There is one equation for each mesh point.)

A few words on the strategy in obtaining the solution to the system of equations is now in order. Eqs. (6-8) may be termed the residual equations whereas Eqs. (9-11) are the relaxation operator equations. Equations of the type (6-8) will apply to each nodal point in the finite difference field. The problem at hand is to reduce systematically the residuals to be acceptably small so that we have an accurate solution to the deflection field.

An iterative procedure is utilized. First the u and v equations [Eqs. (6) and (7)] are set aside and primary attention is focused on the w equations of the type of Eq. (8). Starting with a guess at the w field (which could be assumed to be 0) we reduce the residual at all points to acceptably low values by using the operator of Eq. (11). Next, we hold w constant and solve the u set of equations [the type of Eq. (6) or (1)]. Here, the relaxation procedure is more straightforward because of the linear nature of the relaxation operator in u . When the residuals (or changes of the function) are acceptably low the u field is taken to be tentatively solved and the current values of u and w are subsequently utilized in Eq. (7). When the " v " residuals are acceptably small we proceed back to the w equations again and repeat the process until all residuals or function changes are within a prescribed limit.

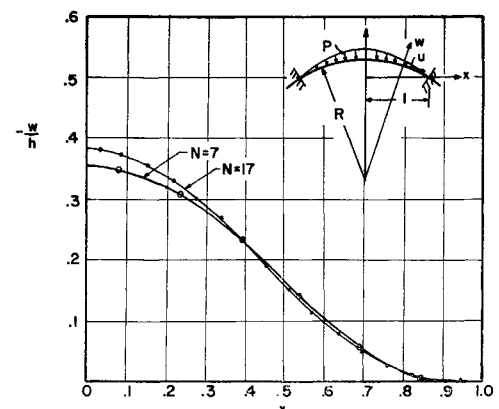


Fig. 5 Geometry of spherical shell under axisymmetry nonuniform load ($p = 0.4 \cos \pi x / 2$) and normal deflection with $N = 7$, and $N = 17$ for $\lambda = 6$, $\nu = \frac{1}{3}$.

(A convergence criterion based on function changes is definitely preferable and is adopted here.)

The procedure just described was similar to the one used by Shaw and Perrone¹⁶ except for the fact that carry-over factors were utilized in the earlier manual analysis. In the present case when resort is being made to a computer and complete orderly sweeps through the finite difference field are conducted it is more direct simply to recalculate the residual at each point just before the residual is reduced. In addition, to accelerate convergence it was demanded that all residuals be 25% over-relaxed (e.g., an initial residual of 100 at a point would be reduced to -25).

The preceding strategy could apply directly to the present problem as well as many other classes of problems of greater or lesser complexity. In the present instance a slight change is necessary occasioned not by difficulties with the solution method but because of finite difference inaccuracies. In the vicinity of the innermost concentric circle of Fig. 2 the finite difference representation of the ∇^4 expression is woefully inaccurate. If the equations were brought down to a lower order, finite difference inaccuracies would no longer be present.† In substance, Famili and Archer¹⁰ have succeeded in achieving just such an effect by introducing a new variable ϕ which is defined as shown in Eq. (14)

$$\nabla^2 w = \phi, \nabla^2 \phi = \nabla^4 w \quad (14)$$

It is only necessary to utilize this modulation for the innermost circle. For the rest of the domain a conventional approach is utilized with no difficulty. For the inner most circle only, the w equation is therefore solved in conjunction with finite difference forms of Eq. (14).

Example Problems

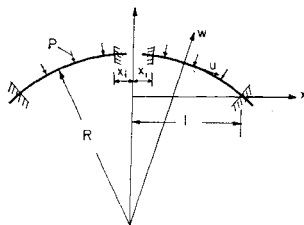
With the technique outlined a broad spectrum of problems are solved ranging from axisymmetric shells of increasing complexity to asymmetrically loaded shells. Although not specifically treated here, shells that are asymmetric with respect to boundaries or other geometric characteristics including thickness variations could be readily considered with no difficulty.

The General Electric Mark II (635) Time Sharing and the Digital Equipment Corporation's PDP 10 Computing Systems were used to carry out the computations. Convergence was not disturbed by poor starting values (usually, 100% in error). Criterion for convergence is that for all nodal points the average absolute percentage change of the function be less than 0.05%.

1. Axisymmetric Problems

With the present displacement type equations it should be obvious that for the axisymmetric case v displacements vanish and only Eqs. (1) and (3) survive. Hence, in the numerical technique employed Eqs. (6) and (8) as well as Eqs. (9) and (11) are the governing ones for the numerical procedure. In other terms, we need only obtain a solution along a radius (or spoke line).

Fig. 6 Geometry of spherical shell with central rigid region.



† This change is necessary for the asymmetric problem but not for the axisymmetric situation. The finite difference errors arise due to terms that have derivatives with respect to θ . For the axisymmetric case these terms fortunately drop out.

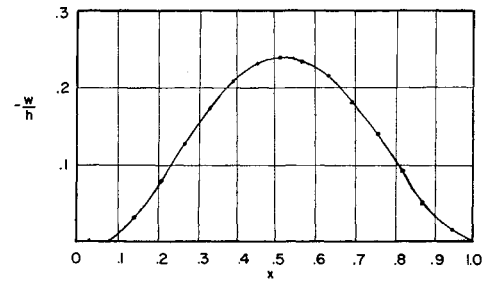


Fig. 7 Normal deflection of shell in Fig. 6 under uniform load ($p = 0.4$) with $x_1 = 1/11$ and $N = 16, \nu = 1/3$.

Solutions are obtained for the uniformly and cosine loaded caps with coarse and fine meshes, Figs. 4 and 5, and for a uniformly loaded cap with a clamped region near the pole, Figs. 6 and 7.

2. Semicircular Loading (Asymmetric)

Normally the asymmetric problem is perhaps an order of magnitude more difficult than the axisymmetric one. As such, the jump from the axisymmetric to asymmetric solution is a significant one.

With the technique being utilized here, however, the asymmetric problem is not, relatively speaking, much more difficult. All that is necessary is to include in the program the residual equation associated with the v displacement, Eq. (7); in addition, many more nodal points are to be treated so that the amount of computer time is much greater.

The first problem treated as a check point is the uniformly-loaded spherical cap. For this case, of course, the axisymmetric solution should suffice to determine the cap response. If we ignore symmetry, however, we can utilize this example as a test case for the asymmetric program. When this was done the asymmetric program converged in approximately five times the computer CPU time to the same solution as for the corresponding axisymmetric problem.

The next problem treated is a nontrivial one, namely, the response of the spherical cap with a semicircular uniform loading as shown in Fig. 8. Also shown in the same figure is the polar coordinate finite difference mesh ($N = 7, M = 10$).

Solutions are obtained at a number of load levels up to and including the instability load. With the technique employed the instability load is calculated within approximately $1/2\%$ accuracy. The deflection profiles along the meridian symmetry line are shown for two load levels (the instability load and about 80% of instability load) in Fig. 9. The load deflection curve for a point near the pole on the symmetry line is presented in Fig. 11.

3. Quarter-Circle Loading (Asymmetric)

A second asymmetric problem treated is that of a spherical cap with loading over a 90° or quarter-circle segment, Fig.

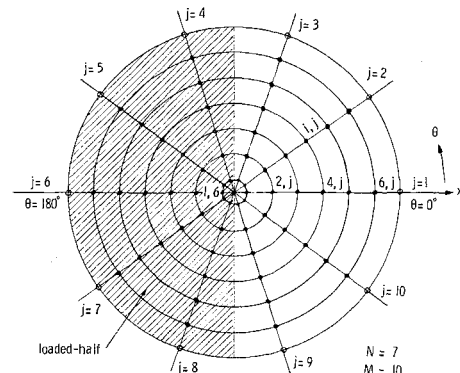


Fig. 8 Finite difference mesh on spherical cap subjected to a uniform load over one-half of surface.

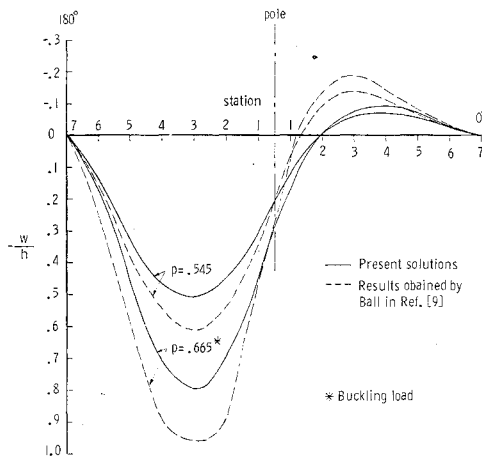


Fig. 9 Deflection profiles along the 0-180° meridian (symmetry line) for half-loaded shell, Fig. 8, with $\lambda = 6$, $\nu = 0.3$.

10. In order to more accurately display the loading chosen, a finer mesh is necessarily selected in the circumferential direction ($M = 12$).

Again solutions are obtained at various load levels up to and including the buckling load. In Fig. 12 the deflection profile along the meridian symmetry line is shown for the buckling load as well as a load level slightly below buckling. It is perhaps of some interest to compare deflection profiles for the same load cases at $p = 0.545$ for the quarter-circle and semicircular-load cases, Figs. 12 and 9. It is surprising to note that the deflection is greater for the cap which has a lesser loading, the quarter-loading case. Obviously, the load some distance away from the point at which deflections are measured has the effect of stiffening the cap, at least along the meridian symmetry line. Although the total loading is half as much as for the half-circle load case, the associated deflections are about 30% greater.

A load deflection curve for a point close to the pole on the meridian symmetry line is superposed on Fig. 11. It is of further interest to note that the buckling load for the quarter-circle loaded cap is lower than that of the semicircular cap by about 20%. On the other hand the maximum deflections which are observed from Figs. 9 and 12 are fairly close at buckling (about 7% difference).

Comparisons with Other Solutions

For some of the solutions obtained in the preceding section on example problems it is possible to make comparisons from the literature with solutions obtained elsewhere. Archer obtained a solution to the uniformly-loaded spherical cap using finite difference techniques and the Reissner shallow shell

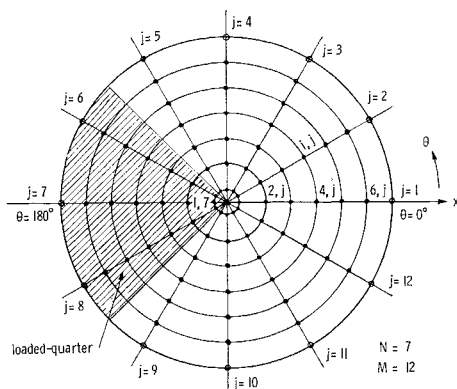


Fig. 10 Finite difference mesh on spherical cap subjected to a uniform load over one-quarter of surface.

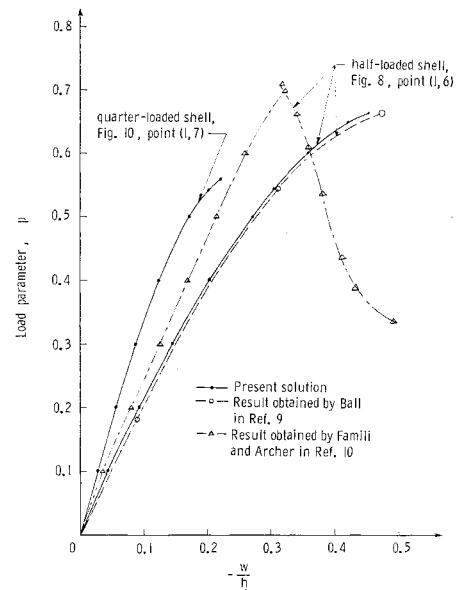


Fig. 11 Load-deflection curves for half and quarter-loaded shells, $\lambda = 6$, $\nu = 0.3$.

equations.¹ He divided the radius into 21 points rather than the 17 used here and his solution is superposed on the current solution in Fig. 4. In view of the fact that a different set of equations has been utilized as well as a completely different solution technique, the comparison is excellent. Because he utilized a set of equations that had a stress function, Archer readily enforced symmetry conditions at the center without, so to speak, going on the other side of the center.¹ In the present case where we have equations in terms of deflection components, symmetry at the apex is satisfied by demanding that w be a symmetric function and u antisymmetric.[§]

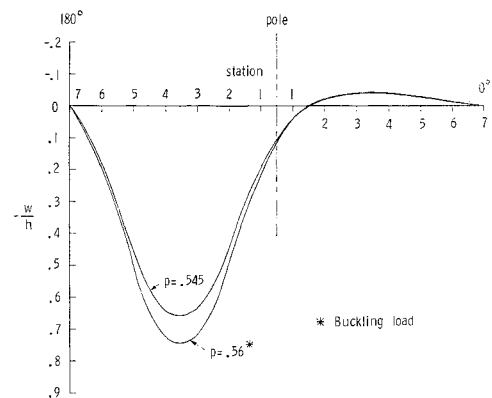


Fig. 12 Deflection profiles along the 0-180° meridian (symmetry line) for quarter-loaded shell, Fig. 10, with $\lambda = 6$, $\nu = 0.3$.

§ In polar coordinates positive u would be radially outward. However, for the inner most circle, if we focus on a particular diametral spoke line running through the circle, positive u displacements would be running in opposite directions. Hence, when setting up the finite difference derivative expressions if we did not recognize the potential paradox we would obtain erroneous derivative values at the center. Specifically, in polar coordinate convention we would obtain a vanishing u derivative at the center with respect to r whereas in point of fact there is definitely a non-zero derivative there related to median surface stretching (associated with the fact that both points are moving in opposite directions). It appears from our examination of the program generated by Famili and Archer¹⁷ that u was inadvertently taken to be symmetric at the center of the cap.

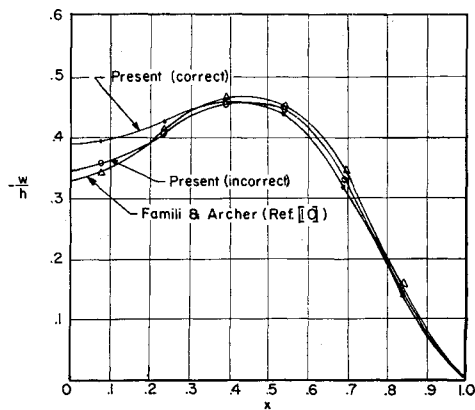


Fig. 13 Comparison of the normal deflection under uniform load using correct and incorrect approaches for u with the results in Ref. 10, for $p = 0.7$, $\nu = \frac{1}{3}$, $N = 7$.

In Famili and Archer's work the spherical cap problem was solved by utilizing the Marguerre equations in terms of displacement quantities and solving the same using a matrix inversion iteration process¹⁰ (Ref. 17 is the original thesis from which the paper, Ref. 10 was excerpted). For the axisymmetric uniform pressure cap problem Famili and Archer obtained a coarse mesh solution having seven points along a radius. In the present work two coarse mesh solutions are obtained and are shown in Fig. 13 along with the results from Ref. 10. In the first case u is taken to be a symmetric function at the center of the shell matching what was utilized in Ref. 10, and in the second case u is taken to be the correct approach. Obviously, when we treat u as symmetric the present solution and that of Famili and Archer are in fairly good agreement, Fig. 13. The effect of introducing the actual antisymmetry at the center causes a deviation as observed in the figure.

It appears that Famili and Archer when solving the semicircular-loaded spherical cap of Fig. 8 may have also neglected to enforce symmetry in the circumferential direction.¹⁰ Along the meridian symmetry line in Fig. 8 it should be apparent that v is an antisymmetric function. For a point along this line a load deflection curve is given in Fig. 11 from the Famili and Archer solution. If v is accepted as being a symmetric function about the symmetry line the current program gives a solution very close to that obtained in Ref. 10. Using the correct antisymmetric requirement at the symmetry line, we obtain the result as shown in Fig. 11 which differs appreciably from the results of Ref. 10.

Using Sanders Equations, Ball also solved the semicircular-loaded cap problem using finite differences in the radial direction and a Fourier expansion in the circumferential direction.⁹ He truncated his Fourier series at four terms to try to simulate in a rather crude way the mesh spacing of Famili and Archer.¹⁰ A load deflection plot that compares all three results for a point on the symmetry line of the semicircular-loaded spherical cap is shown in Fig. 11.

Obviously the present results compare very favorably with Ball's solution. Indeed the buckling loads compare very accurately, being virtually coincident. However, as evidenced by Fig. 9, the deflections for the same load values differ noticeably. In view of the fact that different sets of equations were used, comparisons with Ball's solution in general, may be viewed as quite good.

The quarter-circle loaded cap of Figs. 10 and 12 has not been solved elsewhere in the literature; hence direct comparisons with other solutions are not possible. However, as stated in the previous section, comparisons with the semicircular-loaded cap are of some interest: the lower loaded quarter-circle cap has greater deflections and lower buckling loads than the semicircular-loaded cap.

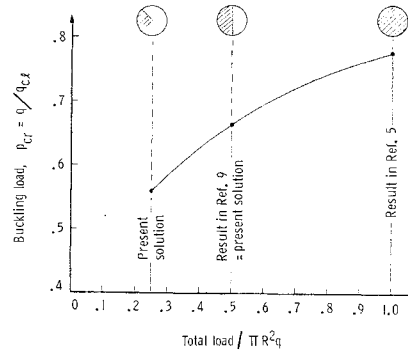


Fig. 14 Buckling load vs total load applied to clamped cap, $\lambda = 6$, $\nu = 0.3$.

Conclusions

In the present paper a nonlinear finite difference relaxation procedure, first utilized many years ago¹⁶ and more recently applied in a somewhat modified form for computer use for flat membrane problems,¹⁴ is here first utilized to solve the general problem of the large deflection response of a spherical cap. The Marguerre equations in terms of displacement functions are replaced by finite difference equivalents, a polar coordinate mesh superposed on the cap domain, and the resulting nonlinear algebraic finite difference equations are solved by a relaxation iteration procedure.

The essential advantage of the solution technique is that it is extremely simple to program and is quite insensitive to starting values as far as convergence is concerned. It is also quite general in application in that it could be applied with equal ease to a very wide spectrum of problems in mechanics as well as applied mathematics. It is also believed that the method is economical as far as the use of computer time is concerned.

The spectrum of spherical shell cap problems that have been solved constitute a varied and complex series of problems ranging from the uniformly-loaded to the asymmetrically loaded spherical cap. The program developed here could apply equally well to determine the response of a spherical cap with no symmetry including irregular boundary conditions, variable thickness, etc.

In general, correlations with solutions obtained elsewhere were either quite good or else deviations occurred which were attributable to specific causes. The buckling load of the shell with semicircular loading obtained here coincided with the value obtained by Ball.⁹ It is of interest to note that the buckling load of the semicircular-loaded cap is appreciably less than that of the fully-loaded cap, and the buckling load of the quarter-circle loaded cap is less than that of the semicircular-loaded cap (Fig. 14). The obvious trend appears to be that the smaller the area over which the load is applied, the lower is the associated buckling pressure.

One of the important points to which attention should be called is the finding that finite difference numerical techniques when applied to polar coordinate type meshes could lead to significant errors especially in the vicinity of the pole. This is particularly true with respect to the ∇^4 operator which is extremely inaccurate even for fine mesh spacing and specifically with respect to derivatives in the circumferential direction. The technique that proved fruitful in avoiding this difficulty is to reduce the order of the equation such as is accomplished here in Eq. (14).

References

- 1 Archer, R. R., "On the Numerical Solution of the Nonlinear Equations for Shells of Revolution," *Journal of Mathematics and Physics*, Vol. 41, 1962, pp. 165-178.
- 2 Wilson, P. E. and Spier, E. E., "Numerical Analysis of Large

Axisymmetric Deformations of Thin Spherical Shells," *AIAA Journal*, Vol. 3, No. 9, Sept. 1965, pp. 1716-1725.

³ Bushnell, D., "Nonlinear Axisymmetric Behavior of Shells of Revolution," *AIAA Journal*, Vol. 5, No. 3, March 1967, pp. 433-439.

⁴ Huang, N. C., "Axisymmetric Dynamic Snap-through of Elastic Clamped Shallow Spherical Shells," *AIAA Journal*, Vol. 7, No. 2, Feb. 1969, pp. 215-220.

⁵ Fitch, J. R. and Budiansky, B., "The Buckling and Post Buckling Behavior of Spherical Caps under Axisymmetric Load," *AIAA Journal*, Vol. 8, No. 4, April 1970, pp. 686-693.

⁶ Weinitschke, H. J., "On Asymmetric Buckling of Shallow Spherical Shells," *Journal of Mathematics and Physics*, Vol. 44, No. 2, June 1965, pp. 141-163.

⁷ Mescall, J., "Large Nonsymmetric Deflections of Thin Shells of Revolution," *Proceedings of the Army Symposium on Solid Mechanics*, Army Materials and Mechanics Research Center, Watertown, Mass., Sept. 1968.

⁸ Leicester, R. H., "Finite Deformations of Shallow Shells," *Journal of the Engineering Mechanics Division of ASCE*, Vol. 94, No. EM 6, Dec. 1968, pp. 1409-1423.

⁹ Ball, R. E., "A Geometrically Nonlinear Analysis of Arbitrarily Loaded Shells of Revolution," CR-909, Jan. 1968, NASA.

¹⁰ Famili, J. and Archer, R. R., "Finite Asymmetric Deforma-

tion of Shallow Spherical Shells," *AIAA Journal*, Vol. 3, No. 3, March 1965, pp. 506-510.

¹¹ Stricklin, J. A., Haisler, W. E., MacDougall, H. R., and Stebbins, F. J., "Nonlinear Analysis of Shells of Revolution by the Matrix Displacement Method," *AIAA Journal*, Vol. 6, No. 12, Dec. 1968, pp. 2306-2312.

¹² Stricklin, J. A. and Martinez, J. E., "Dynamic Buckling of Clamped Spherical Caps under Step Pressure Loadings," *AIAA Journal*, Vol. 7, No. 6, June 1969, pp. 1212-1213.

¹³ Liepins, A. A., "Asymmetric Nonlinear Dynamic Response and Buckling of Shallow Spherical Shells," CR-1376, June 1969, NASA.

¹⁴ Perrone, N. and Kao, R., "A General Relaxation Technique for Solving Nonlinear Problems," Presented at the 12th International Congress of Applied Mechanics, Stanford, Calif., Sept. 1968.

¹⁵ Southwell, R. V., *Relaxation Methods in Theoretical Physics*, Vol. II, The Clarendon Press, Oxford, 1956, pp. 432-494.

¹⁶ Shaw, F. S. and Perrone, N., "A Numerical Solution for the Nonlinear Deflection of Membranes," *Journal of Applied Mechanics*, Vol. 76, June 1954 pp. 117-128.

¹⁷ Famili, J., "On the Vibration, Buckling, and Post Buckling Behavior of Shells of Revolution under Symmetrical and Unsymmetrical Load," Doctoral thesis, 1965, Engineering Div., Case Institute of Technology, Cleveland, Ohio.

DECEMBER 1970

AIAA JOURNAL

VOL. 8, NO. 12

Limit Surfaces for Fibrous Composite Plates

P. V. McLAUGHLIN JR.*
University of Illinois, Urbana, Ill.

AND

S. C. BATTERMAN†
University of Pennsylvania, Philadelphia, Pa.

The limit theorems of perfect plasticity and their recent extensions are used to derive limit surfaces for representative structural elements of fibrous composite plates, which are composed of long, elastic, perfectly plastic fibers site bonded or imbedded in a matrix of negligible strength. The limit surfaces are presented in the form of equations in six-dimensional generalized stress space and are completely analogous to yield surfaces for perfectly plastic structures and materials. The effects of fiber orientation geometry, fiber yielding, fiber buckling, and pullout of the fibers from the remaining structure are included in the theory and illustrated with an example.

Introduction

IN a recent paper,¹ the basic theory and technique of computing limit surfaces for long-fiber composite materials was presented. It was shown that membranes composed of long, elastic, perfectly-plastic fibers, which were site bonded or imbedded in a matrix of negligible strength, could be treated by limit analysis techniques^{2,3} to obtain limit surfaces for all combinations of in-plane loading. These limit surfaces are completely analogous to yield surfaces for per-

fectly plastic materials, and include the effect of fiber buckling and pullout of fibers from the remaining structure in addition to perfectly plastic flow.²

The basic tools used in Ref. 1 were the limit theorems³ that have recently been extended to encompass phenomena other than perfect plasticity.² For composites, fiber buckling and pullout are admissible limit phenomena as long as they occur under constant axial load (Fig. 1). Furthermore, structural collapse that occurs as a result of any combination of acceptable limit phenomena can be handled within the framework of limit analysis. The extended limit theorems are used herein to develop equations for limit surfaces for representative structural elements of fibrous composite plates having arbitrary fiber orientation and density, and which exhaust their load-carrying capacity due to one or any combination of perfectly plastic flow of fibers, elastic buckling of fibers,^{4,5} and pullout of fibers from the remaining structure. Not only are these surfaces exact for fibrous plates that are site bonded or impregnated with a matrix having negligible strength, but they are also a rigorous lower bound to the limit surfaces for fibrous plates having a matrix whose strength is not negligible. The results are, therefore, applicable to both high- and low-

Received January 19, 1970; revision received May 27, 1970. This work is based in part on a dissertation submitted to the University of Pennsylvania by P. V. McLaughlin Jr. in partial fulfillment of the requirements for the degree of Ph.D. P. V. McLaughlin Jr. is grateful for the support of the Scott Paper Company, and S. C. Batterman gratefully acknowledges the support of the National Science Foundation, the Advanced Research Projects Agency, and the Pennsylvania Science and Engineering Foundation while making this study.

* Assistant Professor of Theoretical and Applied Mechanics; formerly, Senior Research Project Engineer, Scott Paper Company, Philadelphia, Pa.

† Associate Professor of Engineering Mechanics.